FULL PAPER

# High-Performance Electrofluorochromic Devices Based on Electrochromism and Photoluminescence-Active Novel Poly(4-Cyanotriphenylamine)

*Jia-Hao Wu and Guey-Sheng Liou**

**A novel electrochromism (EC) and photoluminescence (PL)-active poly(4-cyanotriphenylamine) (CN-PTPA) is prepared by oxidative coupling polymerization from 4-cyanotriphenylamine (CN-TPA) using $FeCl_3$ as an oxidant. The high-performance electrofluorochromic (EFC) devices using CN-PTPA thin film with photoluminescent quantum yield of 21.9% as active layer are readily fabricated and reveal the highest fluorescent contrast ratio ($I_{off}/I_{on}$) of 242 between the fluorescent (neutral) state and the non-fluorescent (oxidized) state, rapid response time shorter than 0.4 s, and excellent EFC stability longer than 9000 s. Furthermore, by introducing viologen into electrolyte as a counter EC layer for charge balance, the resulting EFC device exhibits notable improvement in reducing oxidation potential (from 2.30 V to 1.55 V) and switching recovery time (from 78 to 38 s) with enhanced fluorescent contrast ratio during pulse on/off multi-cyclic scanning. These results demonstrate that incorporation of the EC and PL-active CN-PTPA is a facile and feasible approach to prepare highly efficient EFC devices.**

## 1. Introduction

Controllable fluorescence switching materials have attracted significant attention for the potential applications including sensors[1] especially in bio-issue,[2] optical memory devices,[3] logic gates,[4] vivo imaging,[5] and displays.[6] The changes of fluorescent intensity could be triggered by different types of external conditions, such as voltage,[7] temperature,[8] pH,[9] and light.[3a,9,10] Among them, electrically driven is a facile approach to achieve the demand. Electrofluorochromism (EFC) deals with the reversible optical switching between high (OFF) and low (ON) fluorescence intensity states via redox-driven electric potentials. The EFC behavior could be attributed to two kind of mechanism. One is redox active fluorophore switched from light to dark via intrinsic electron transfer during redox process, such as tetrazine[11] and triphenylamine (TPA).[12] The other is by introducing redox active moiety as a quencher to induce energy transfer from phorophore during redox process.[13] A high-performance EFC device should includes the following characteristics: high photoluminescent (PL) efficiency, high contrast, long-term stability, and rapid response time. Therefore, the design of materials with smarter molecular structures is essential for modern optoelectronic applications. Since 2006, several EFC devices have been fabricated and investigated including small organic molecules,[11,14] inorganic materials,[13d,15] conjugated polymers,[1b,13a] high-performance polymers,[12,16] and hybrids.[17] However, emerged materials could not comprise all the characteristics mentioned above yet to achieve a high-performance EFC device.

TPA derivatives are promising materials for optoelectronic applications such as hole-transporters, light-emitters, photovoltaic, electrochromic, and memory devices due to their outstanding photo- and redox-active properties.[18] Recently, we reported two TPA-based high-performance polymers exhibiting high PL efficiency and high contrast ratio ($I_{off}/I_{on}$) in EFC device applications.[12] However, some crucial characteristics for practical applications including response time and long-term switching stability have not been well attained. In light of the importance of these properties, we are interested in preparing conjugated polymers with higher charge-mobility and electrochemical stability to demonstrate the feasibility for obtaining high-performance EFC with all the critical demands described above.

In this article, herein we prepared the conjugated electrochromism (EC) and PL-active TPA-based polymer, poly(4-cyanotriphenylamine) (**CN-PTPA**), and the corresponding non-congugated polyimide **CN-PI** with the same 4-cyanotriphenylamine (**CN-TPA**) moiety to demonstrate the effect of conjugated and isolated structures on EFC behaviors. Furthermore, the modified two-electrode devices were also fabricated and investigated by introducing heptyl viologen (HV)[19] into electrolyte as counter EC layer for charge balance to reduce driving potential and response time, and to intensify other properties.

J.-H. Wu, Prof. G.-S. Liou
Functional Polymeric Materials Laboratory
Institute of Polymer Science and Engineering
National Taiwan University
1 Roosevelt Road, 4th Sec, Taipei 10617, Taiwan
E-mail: gsliou@ntu.edu.tw

DOI: 10.1002/adfm.201401608

## 2. Results and Discussion

### 2.1. Basic Properties of CN-PTPA

**CN-PTPA** (**Figure 1**a) could be readily prepared by oxidative coupling polymerization from **CN-TPA** using $FeCl_3$ as an oxidant.

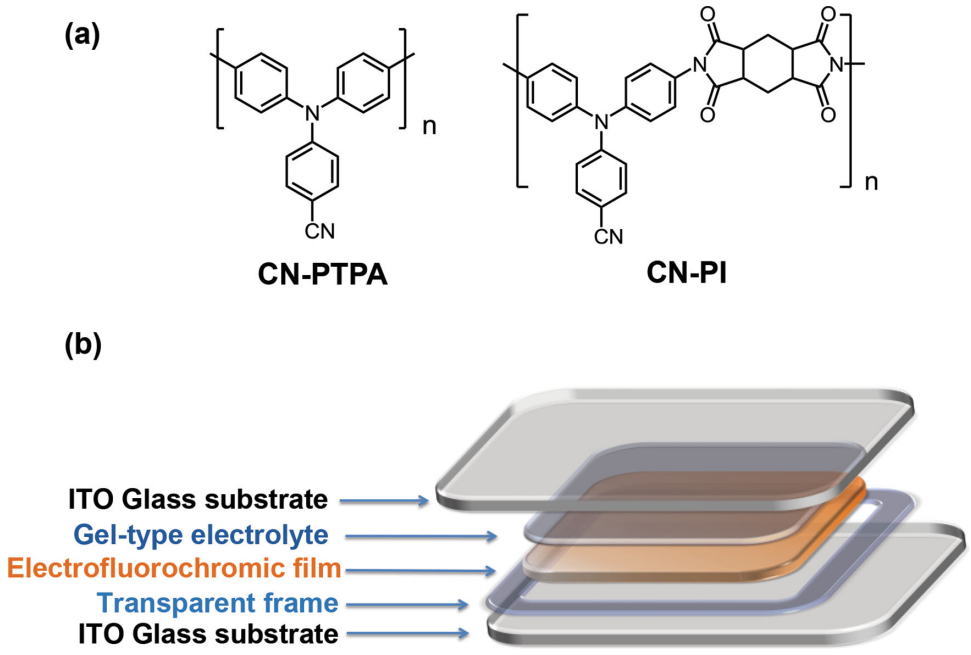


**Figure 1.** a) Chemical structures of **CN-PTPA** and **CN-PI**, b) schematic diagram of EFC devices based on the polymers.

The molecular weight and solubility behavior of the polymer were summarized in Table S1. **CN-PTPA** exhibits excellent solubility even in less polar solvent that is beneficial to the practical applications by spin-coating and inkjet-printing processes. The thermal properties of **CN-PTPA** were investigated by TGA (Figure S1, Supporting Information) and DSC (Figure S2, Supporting Information), and the results were summarized in Table S2 (Supporting Information). The **CN-PTPA** exhibited high glass-transition temperature (Tg) of 278 °C and excellent thermal stability without significant weight loss up to 620 °C with char yield of 75% at 800 °C under nitrogen atmosphere.

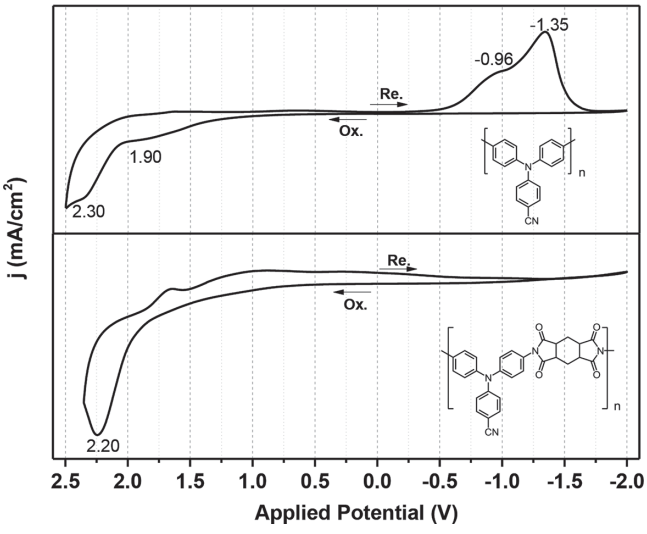


**Figure 2.** Cyclic voltammetry diagrams of **CN-PTPA** and **CN-PI** devices at a scan rate of 50 mV $s^{-1}$.

### 2.2. Electrochemical and Electrochromic Properties of the EFC Devices

The electrochemical behavior of **CN-PTPA** and **CN-PI** devices was investigated by cyclic voltammetry (CV) shown in **Figure 2**. The CV diagram of **CN-PTPA** film on an ITO-coated glass substrate using 0.1 M tetrabutylammonium perchlorate (TBAP)/$CH_3CN$ as supporting electrolyte in a nitrogen atmosphere was also dipicted in Figure S3 (Supporting Information) for comparison. **CN-PTPA** device revealed two oxidative peak at 1.90 and 2.30V because the repeat units of **CN-PTPA** could also be regarded as tetraphenylbenzidine (TPB) moiety dimerized from TPA.[20] The typical spectroelectrochemical spectra of **CN-PTPA** was presented in **Figure 3**, and the electrochromic (EC) behavior was reversible. The EFC device is transparent and colorless at the neutral form (0 V), upon oxidation (increasing applied voltage from 0 to 1.90 V), the intensity of the absorption peak at 362 nm (0 V, neutral form) characteristic of triarylamine gradually decreased, while new peaks around 488 and 733 nm in visible-light region associating with strong color changes and a broad absorption band around 1700 nm characteristic of inter-valence charge-transfer (IV-CT) gradually increased in intensity due to the formation of cation radical of **CN-PTPA** at semi-oxidized state (Figure S4, Supporting Information). When the potential was adjusted to more positive values (1.90–2.30 V) corresponding to the full-oxidized state, the intensity of IV-CT band decreased while the absorption peaks at both 488 and 733 nm were intensified. Meanwhile, the color of the EFC device changed from colorless ($L^*$, 97.31; $a^*$, –0.23; $b^*$, 1.20) to brown ($L^*$, 70.63; $a^*$, 17.77; $b^*$, 29.26), and then to blue ($L^*$, 40.02; $a^*$, –4.91; $b^*$, –9.33) (Figure 3c,d), revealing very high optical transmittance contrast ($\Delta\%T$) of 82% at 733 nm.

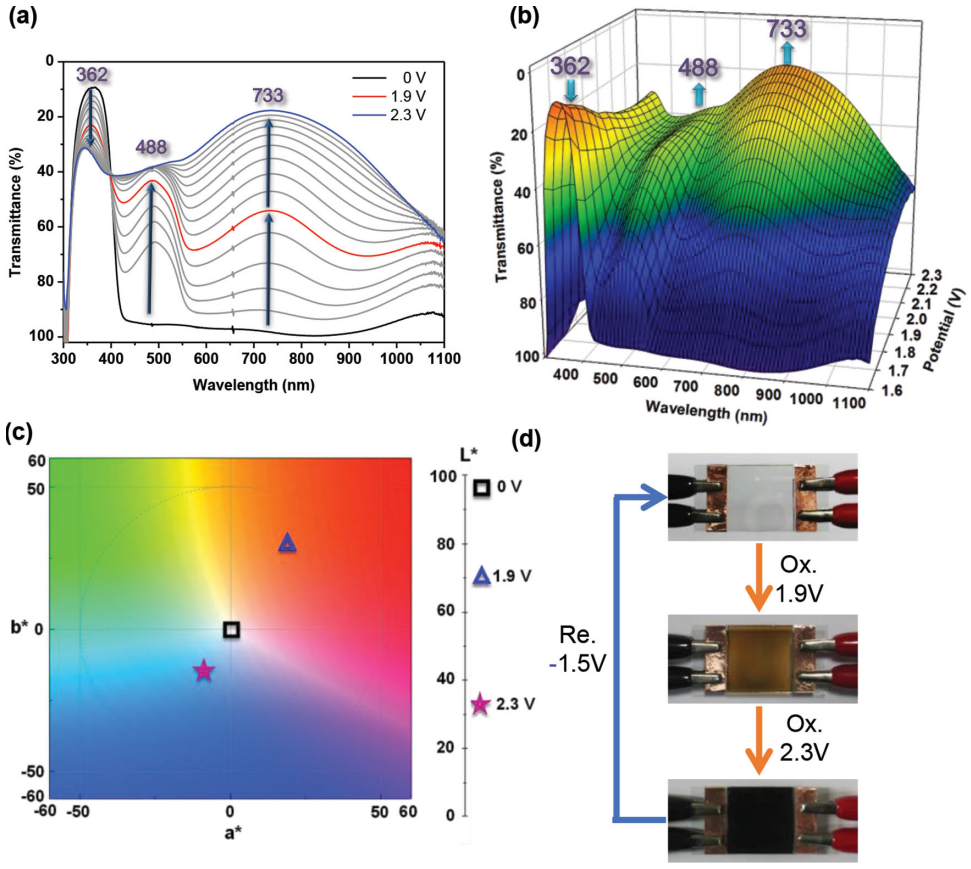


**Figure 3.** a) UV–Vis spectra, b) 3-D spectroelectrochemical diagram, c) CIE 1976 color diagram, and d) EC behavior of **CN-PTPA** device (polymer film 200 ± 10 nm in thickness).

### 2.3. Electrofluorochromic Properties of the EFC Devices

**CN-PTPA** showed high PL quantum efficiency of 21.9% in solid film state, and emitted bluish-green light under UV irradiation as shown in Figure S5, The photophysical behavior of **CN-PTPA** was tabulated in **Table 1**. The PL intensity changes of EFC device at different applied positive potentials were depicted in **Figure 4**. The typical PL spectra and three-dimensional intensity-wavelength-applied potential correlations of **CN-PTPA** device were summarized in Figure 4a,b, respectively. Upon applying positive voltage from 0 to 1.90 V, the fluorescence of **CN-PTPA** device was quenched to dark as applied potential around 1.50 V, then almost extinguished at 1.90 V (Figure 4c) due to the cation radical of **CN-PTPA** with an absorption band at around 488 nm, acting as an effective fluorescence quencher during oxidative process. The PL intensity could be retained when the potential was subsequently set back to –1.50 V. In addition, it is worthy to be mentioned that the EFC device derived from **CN-PTPA** revealed the highest PL contrast ratio ($I_{off}/I_{on}$: between neutral fluorescent state and oxidized non-fluorescent state) of 242 to the best of our knowledge.[21]

**Table 1.** Optical Properties of **CN-PTPA**.

| Polymer | NMP (10 μM) solution | | | Solid Film | | | |
|---|---|---|---|---|---|---|---|
| | $\lambda_{abs}$ [nm] | $\lambda_{em}$ [nm] | $\Phi_{PL}$ [%] | $\lambda_{onset}$ [nm] | $\lambda_{abs}$ [nm] | $\lambda_{em}$ [nm] | $\Phi_{PL}$ [%] |
| **CN-PTPA** | 364 | 473 | 11.7 | 410 | 362 | 470 | 21.9 |

The redox cycles were carried out for EFC devices of **CN-PTPA** and **CN-PI** to elucidate the response behavior during the fluorescence switching procedure (**Figure 5**). The devices exhibited reversible fluorescence switching by repetitive applied potential between oxidized (non-fluorescent) state and neutral (fluorescent) state. The fluorescence response time estimated at 90% of the full switching of **CN-PTPA** and **CN-PI** was monitored at 470 nm and 435 nm, respectively (Figure 5a,b), and the **CN-PTPA** device showed notably shorter response time of 0.4 s than **CN-PI** of 4.6 s for switching to oxidized state. This phenomenon maybe could be ascribed to the **CN-PTPA** having more conjugated structure than the isolated **CN-PI**, resulting in enhanced intra-molecule charge transport ability as depicted in **Figure 6**. In addition, the response time dependent behavior of PL contrast ratio was also demonstrated via decreasing contrast ratio both from 242 to 44 for **CN-PTPA** and 192 to 5 for **CN-PI** by reducing the switching cyclic time from 360 s to 10 s, respectively (Figure 5c,d). Furthermore, long-term stability and reversibility of the resulting EFC devices were also investigated by measuring the PL intensity as a function of switching cycles shown in **Figure 7**. The recovery of EFC devices of **CN-PTPA** and **CN-PI** was 99% and 95% after 300 and 100 cycles, respectively. The excellent EFC stability of **CN-PTPA** attributed to the

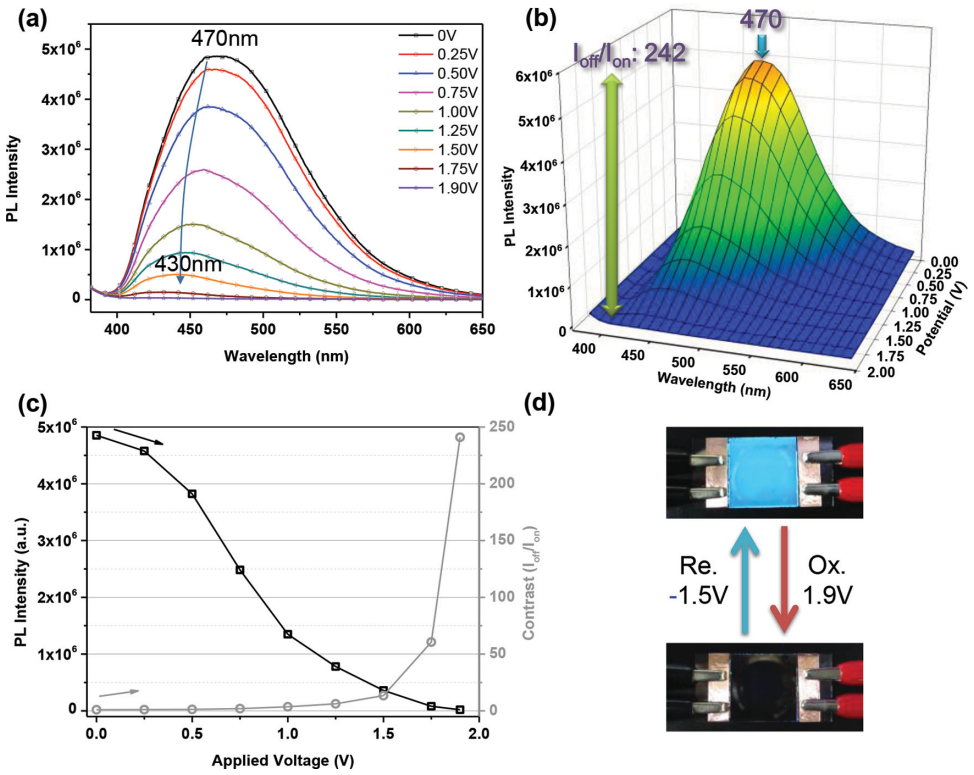


**Figure 4.** a) PL spectra, b) 3-D EFC diagram, c) applied votage vs PL intensity and contrast diagram, and d) EFC behavior of **CN-PTPA** device (polymer film 200 ± 10 nm in thickness).

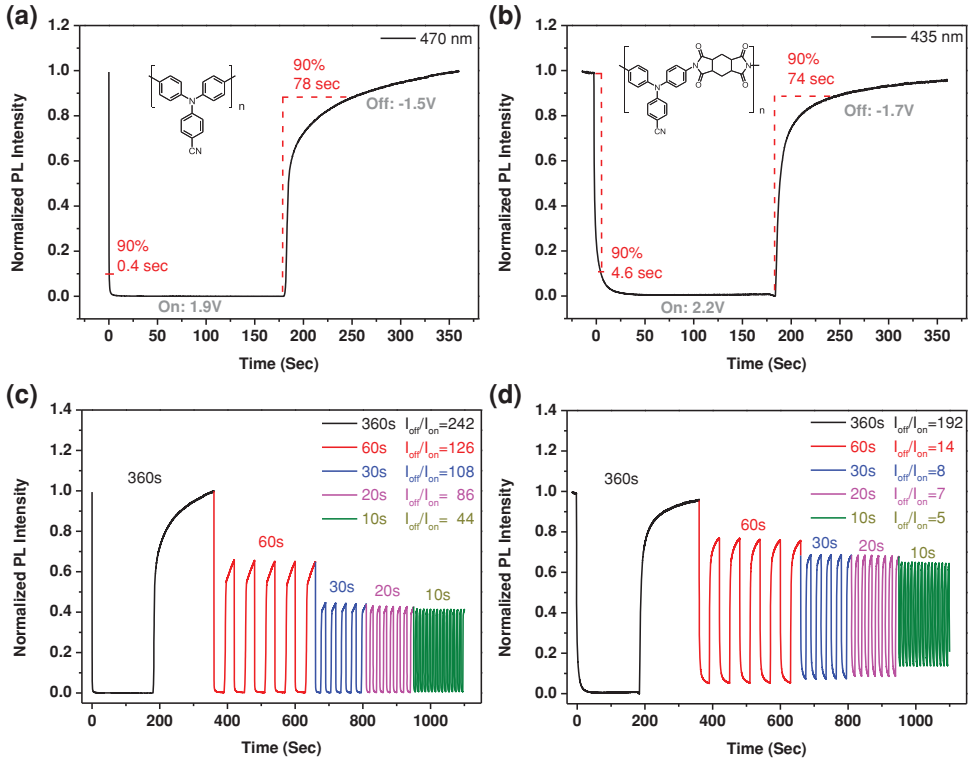


**Figure 5.** Estimation of fluorescence switching time of a) **CN-PTPA** between 1.9 V and –1.5 V monitored at 470 nm ($l_{ex}$ = 362 nm), and b) **CN-PI** between 2.2 V and –1.7 V monitored at 435 nm ($l_{ex}$ = 326 nm). Fluorescence switching responses of c) **CN-PTPA** and d) **CN-PI** at different step cycle times of 360, 60, 30, 20, and 10 s.

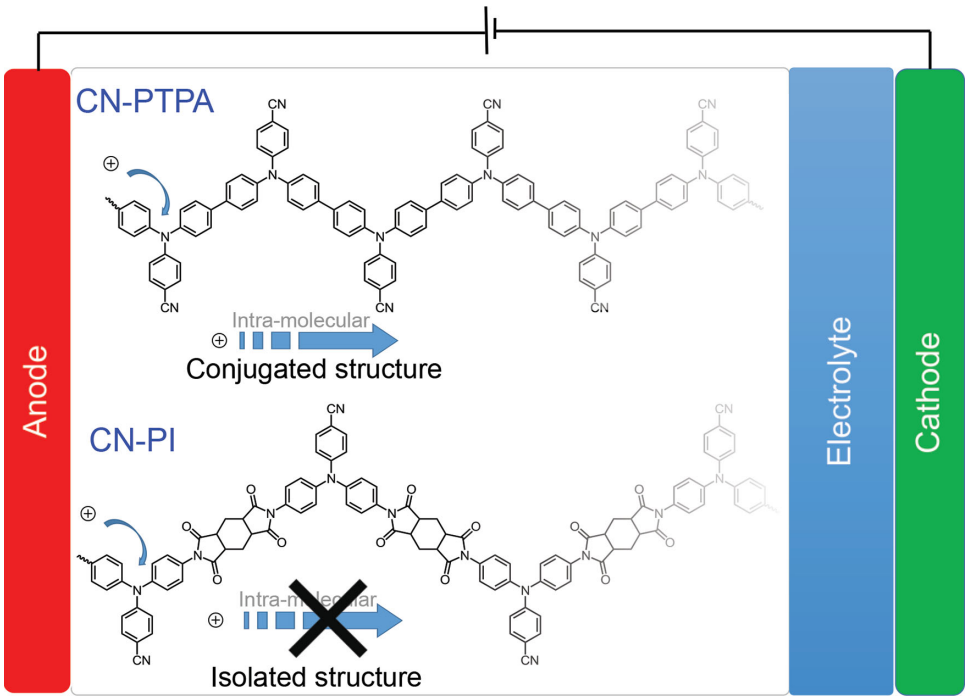


**Figure 6.** Schematic diagram of charge transport of EFC devices from different polymer structures.

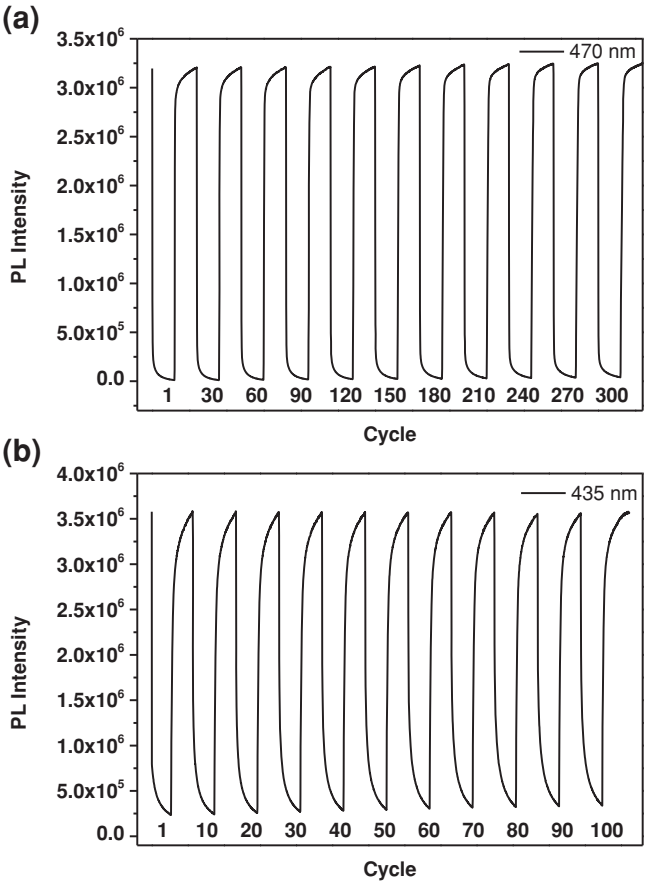


**Figure 7.** EFC switching of a) **CN-PTPA** and b) **CN-PI** with a cycle time of 30 s.

lower oxidation potential resulted in almost no decay when compared with the case of **CN-PI**.

### 2.4. The Effect of HV as Counter Layer on Charge Balance

The CV of **CN-PTPA**/HV device was also prepared and investigated shown in **Figure 8**, and revealed a reversible oxidation redox with much lower oxidative voltage (1.55 V) than the corresponding device (2.30 V) without HV. This phenomenon could be ascribed to $HV^{2+}$ having the capability to accept electrons from TPA moieties during oxidative process and then the resulted $HV^{+}$ could donate electrons back to $TPA^{+}$ during

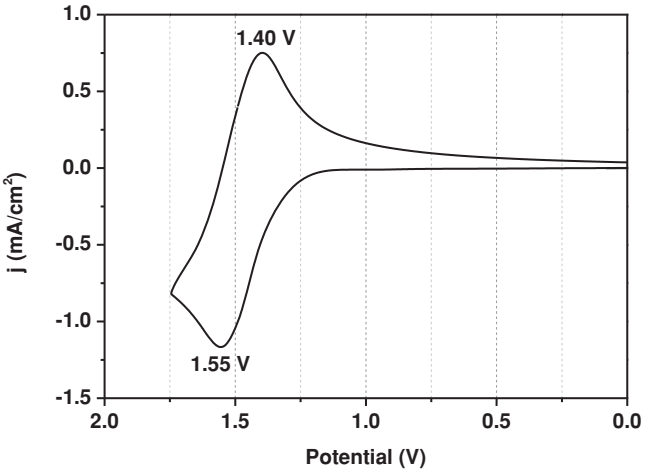


**Figure 8.** Cyclic voltammetric diagram of **CN-PTPA**/HV device at a scan rate of 50 mV/s.

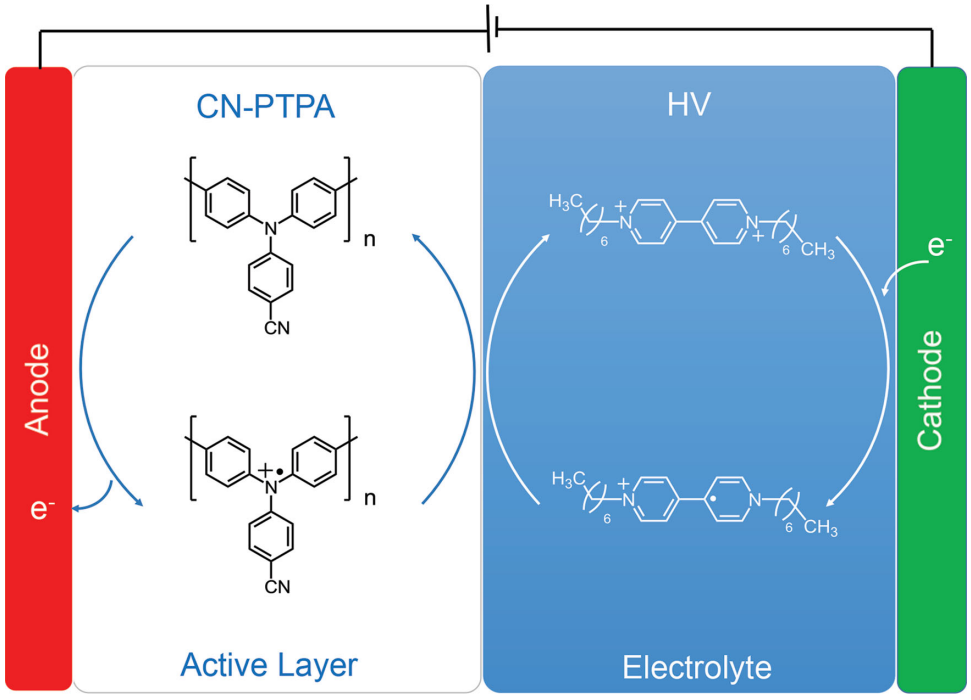


**Figure 9.** Working principle of **CN-PTPA**/HV EFC device.

reducing process (**Figure 9**). The spectroelectrochemical spectra were measured and presented in Figure S6 (Supporting Information). The UV–Vis spectrum of **CN-PTPA**/HV device at the neutral form (0 V) showed similar absorption pattern to the device without HV. However, a broad absorption peak was gradually increased and intensified due to the combination of structural changes both from TPA to $TPA^+$ and $HV^{2+}$ to $HV^+$ at the same time during applied potential from 0 V to 1.6 V.

EFC behavior of **CN-PTPA**/HV device was also investigated and depicted in **Figure 10**. Upon applying potential from 0

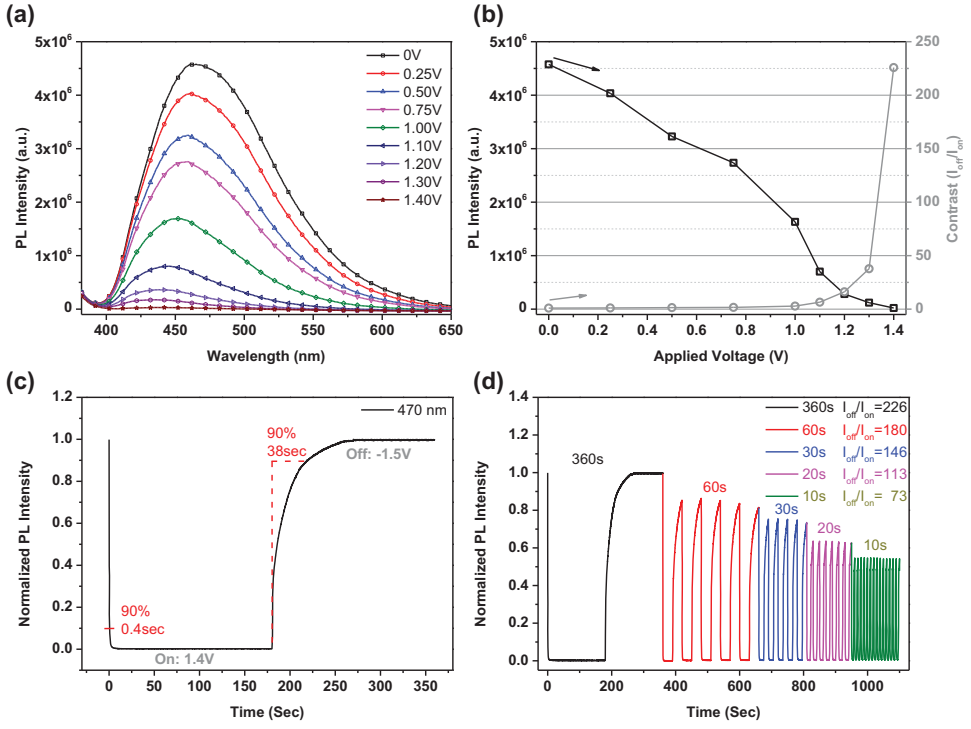


**Figure 10.** a) PL spectra, b) applied voltage vs PL intensity and contrast diagram, c) switching time test, and d) PL intensity and contrast of **CN-PTPA**/HV device under multi-cycle scanning at different step cycle time.

to 1.40 V, the fluorescence was quenched to dark when the potential was at around 1.20 V and almost extinguished at 1.40 V, resulted in very high PL contrast ratio of 226 shown in Figure 10a,b, respectively. Furthermore, the fluorescence switching responses of **CN-PTPA**/HV revealed quenching time of 0.4 s and recovery time of 38 s monitored at 470 nm between 1.40 V and –1.50 V depicted in Figure 10c, which was much less than the corresponding device without HV. Moreover, the reversibility of fluorescence intensity and PL contrast ratio of **CN-PTPA**/HV device under multi-cycle scanning with different step cycle time were summarized in Figure 10d. The redox pulse-cyclic test results demonstrate the effect of HV-containing electrolyte on the performance of EFC devices. Thus, high-performance EFC devices comprising excellent long-term stability, prompt switching response, and higher PL contrast ratio could be readily achieved due to charge balance between the counter material HV and **CN-PTPA**.

## 3. Conclusion

The high-perforemence EFC devices could be successfully fabricated from electrochromism and photoluminescence active novel **CN-PTPA**. The EFC devices of **CN-PTPA** exhibited excellent reversibility over 9000 s, rapid response time less than 0.4 s over the oxidation process, and the highest PL contrast ratio ($I_{off}/I_{on}$) of 242 between fluorescent neutral state and non-fluorescent oxidized state to the best of our knowledge. In addition, by introducing HV into the electrolyte as charge balance agent, the obtained EFC devices not only could reduce the oxidative potential but also the recovery time from oxidized to neutral states, thus the performance could be further enhanced than ever. These results demonstrate that the novel EC and PL-active **CN-PTPA** is a crucial and promising material for attaining to high-perforemence EFC devices.

## 4. Experimental Section

*Materials*: **CN-PI** and **CN-PTPA** were prepared according to the previously reported procedures,[21] and the synthesis route of **CN-PTPA** was depicted in **Scheme S1**. Heptyl viologen tetrafluoroborate $HV(BF_4)_2$ was prepared as follows: 1.00 g $HVBr_2$ was dissolved in 10 mL DI water and dropped in 10 mL saturated $NaBF_4$ aqueous solution. After mixing, the white solid $HV(BF_4)_2$ was obtained after filtration. The crude product was purified by recrystallization from ethanol. All other reagents were used as received from commercial sources.

*Fabrication of the Electrofluorochromic Devices*: EFC polymer films were prepared by coating solution of the polymers (**CN-PTPA**: 25 mg/mL in $CHCl_3$; **CN-PI**: 50 mg/mL in DMAc) onto an ITO glass substrate (20 mm × 30 mm × 1 mm, 5 Ω/square) as depicted in Figure 1b. The ITO glass used for EFC device was cleaned by ultrasonication with water, acetone, and isopropanol each for 15 min. The polymer was spin-coated onto an active area (20 mm × 20 mm) then dried under vacuum. A gel electrolyte based on poly(methyl methacrylate) (PMMA) (Mw: 120,000) and $LiClO_4$ was plasticized with propylene carbonate (PC) to form a highly transparent and conductive gel. PMMA (3 g) was dissolved in PC (5 g), and $LiClO_4$ (0.3 g) was added to the polymer solution as supporting electrolyte. HV electrolyte in this study was prepared as follows: PMMA (3 g) was dissolved in PC (5 g), and then $LiBF_4$ (0.3 g) and $HV(BF_4)_2$ (0.15 g) were added to the polymer solution as 0.05M HV electrolyte. The gel electrolyte was spread on the polymer-coated side of the electrode, and then two electrodes were sandwiched. Finally, a silicone sealant was used to seal the device.

*Measurements*: The inherent viscosities were determined at 0.5 g/dL concentration using Tamson TV-2000 viscometer at 30 °C. Gel permeation chromatographic (GPC) analysis was carried out on a Waters chromatography unit interfaced with a Waters 2410 refractive index detector and was calibrated with polystyrene standards. Two Waters 5 μm Styragel HR-2 and HR-4 columns (7.8 mm I. D. × 300 mm) were connected in series using NMP as the eluent at a flow rate of 0.5 ml/min at 40 °C. DSC analyses were performed on a TA Instruments Q20 in flowing nitrogen (50 $cm^3$/min) at a heating rate of 20 °C/min. Thermogravimetric analysis (TGA) was conducted with a TA Instruments Q50 in flowing nitrogen or air (flow rate = 60 $cm^3$/min) at a heating rate of 20 °C/min. Spectroelectrochemical experiments were recorded on a Hewlett-Packard 8453 UV–Visible diode array spectrometer. Colorimetric measurements were obtained using JASCO V-650 spectrophotometer and the results are expressed in terms of lightness ($L^*$) and color coordinates ($a^*$, $b^*$). Ultraviolet-visible-near-infrared (UV–Vis–NIR) spectra of the polymer films were recorded on a Hitachi U-4100 spectrometer. Cyclic voltammetry (CV) was performed with a CH Instruments 611B electrochemical analyzer and conducted by using a two-electrode device (polymer films area about 2.0 cm × 2.0 cm), or a conventional liquid cell in which ITO (polymer films area about 0.5 cm × 1.2 cm) was used as a working electrode and a platinum wire as an auxiliary electrode at a scan rate of 50 mV/s against a Ag/AgCl as reference electrode in anhydrous $CH_3CN$, using 0.1 M of TBAP as a supporting electrolyte in nitrogen atmosphere. Photoluminescence (PL) spectra were measured with Fluorolog-3 spectrofluorometer. The thickness of the polymer thin film was measured by alpha-step profilometer (Kosaka Lab., Surfcorder ET3000, Japan).

## Supporting Information

Supporting Information is available from the Wiley Online Library or from the author.

## Acknowledgements

The authors gratefully acknowledge the National Science Council of Taiwan for the financial support.

Received: May 19, 2014
Revised: June 24, 2014
Published online: August 22, 2014

[1] a) J. You, J. Kim, T. Park, B. Kim, E. Kim, *Adv. Funct. Mater.* **2012**, *22*, 1417; b) G. Ding, H. Zhou, J. Xu, X. Lu, *Chem. Commun.* **2014**, *50*, 655; c) S. J. Toal, K. A. Jones, D. Magde, W. C. Trogler, *J. Am. Chem. Soc.* **2005**, *127*, 11661.

[2] a) Y. Lee, S. Park, S. W. Han, T. G. Lim, W. G. Koh, *Biosens. Bioelectron.* **2012**, *35*, 243; b) H. Kobayashi, P. L. Choyke, *Acc. Chem. Res.* **2011**, *44*, 83.

[3] a) C. Yun, J. You, J. Kim, J. Huh, E. Kim, *J. Photochem. Photobio. C: Photochem. Rev.* **2009**, *10*, 111; b) C. Yun, S. Seo, E. Kim, *J. Nanosci. Nanotechnol.* **2010**, *10*, 6850; c) R. A. Bissell, A. P. De Silva, H. Q. N. Gunaratne, P. L. M. Lynch, G. E. M. Maguire, K. Sandanayake, *Chem. Soc. Rev.* **1992**, *21*, 187; d) W. R. Browne, M. M. Pollard, B. de lange, A. Meetsma, B. L. Feringa, *J. Am. Chem. Soc.* **2006**, *128*, 12412; e) S. K. Ray, S. Maikap, W. Banerjee, S. Das, *J. Phys. D: Appl. Phys.* **2013**, *46*, 153001.

[4] a) A. P. de Silva, N. D. McClenaghan, *Chem. Eur. J.* **2004**, *10*, 574; b) A. Credi, *Angew. Chem. Int. Ed.* **2007**, *46*, 5472; c) P. Remon,

M. Balter, S. Li, J. Andreasson, U. Pischel, *J. Am. Chem. Soc.* **2011**, *133*, 20742; d) A. P. de Silva, S. Uchiyama, *Top. Curr. Chem.* **2011**, *300*, 1.

[5] a) Y. Kim, H. Y. Jung, Y. H. Choe, C. Lee, S. K. Ko, S. Koun, Y. Choi, B. H. Chung, B. C. Park, T. L. Huh, I. Shin, E. Kim, *Angew. Chem. Int. Ed.* **2012**, *51*, 2878; b) L. Zhu, W. Wu, M. Q. Zhu, J. J. Han, J. K. Hurst, A. D. Q. Li, *J. Am. Chem. Soc.* **2007**, *129*, 3524; c) T. Grotjohann, I. Testa, M. Leutenegger, H. Bock, N. T. Urban, F. Lavoie-Cardinal, K. I. Willig, C. Eggeling, S. Jakobs, S. W. Hell, *Nature* **2011**, *478*, 204.

[6] a) J. Kim, J. You, E. Kim, *Macromolecules* **2010**, *43*, 2322; b) Y. Kim, Y. Kim, S. Kim, E. Kim, *ACS Nano* **2010**, *4*, 5277; c) A. Koppelhuber, O. Bimber, *Opt. Express* **2013**, *21*, 4796.

[7] P. Audebert, F. Miomandre, *Chem. Sci.* **2013**, *4*, 575.

[8] a) R. Abbel, R. van der Weegen, W. Pisula, M. Surin, P. Leclere, R. Lazzaroni, E. W. Meijer, A. P. H. J. Schenning, *Chem. Eur. J.* **2009**, *15*, 9737; b) Y. Sagara, T. Kato, *Angew. Chem. Int. Ed.* **2011**, *50*, 9128.

[9] C. Li, Y. Zhang, J. Hu, J. Cheng, S. Liu, *Angew. Chem. Int. Ed.* **2010**, *49*, 5120.

[10] J. K. Sun, L. X. Cai, Y. J. Chen, Z. H. Li, J. Zhang, *Chem. Commun.* **2011**, *47*, 6870.

[11] S. Seo, Y. Kim, Q. Zhou, G. Clavier, P. Audebert, E. Kim, *Adv. Funct. Mater.* **2012**, *22*, 3556.

[12] H. J. Yen, G. S. Liou, *Chem. Commun.* **2013**, *49*, 9797.

[13] a) C. P. Kuo, C. N. Chuang, C. L. Chang, M. K. Leung, H. Y. Lian, K. C. W. Wu, *J. Mater. Chem. C* **2013**, *1*, 2121; b) D. C. Magri, M. C. Fava, C. J. Mallia, *Chem. Commun.* **2014**, *50*, 1009; c) R. Zhang, Z. Wang, Y. Wu, H. Fu, J. Yao, *Org. Lett.* **2008**, *10*, 3065; d) F. Miomandre, R. B. Pansu, J. F. Audibert, A. Guerlin, C. R. Mayer, *Electrochem. Commun.* **2012**, *20*, 83.

[14] a) D. Canevet, M. Salle, G. Zhang, D. Zhang, D. Zhu, *Chem. Commun.* **2009**, 2245; b) F. Montilla, R. Esquembre, R. Gomez, R. Blanco, J. L. Segura, *J. Phys. Chem. C* **2008**, *112*, 16668; c) Y. Kim, E. Kim, G. Clavier, P. Audebert, *Chem. Commun.* **2006**, 3612.

[15] a) Y. X. Yuan, Y. Chen, Y. C. Wang, C. Y. Su, S. M. Liang, H. Chao, L. N. Ji, *Inorg. Chem. Commun.* **2008**, *11*, 1048; b) H. X. Gu, L. H. Bi, Y. Fu, N. Wang, S. Q. Liu, Z. Y. Tang, *Chem. Sci.* **2013**, *4*, 4371.

[16] S. Seo, Y. Kim, J. You, B. D. Sarwade, P. P. Wadgaonkar, S. K. Menon, A. S. More, E. Kim, *Macromol. Rapid Commun.* **2011**, *32*, 637.

[17] L. Jin, Y. Fang, D. Wen, L. Wang, E. Wang, S. Dong, *Acs Nano* **2011**, *5*, 5249.

[18] a) A. Iwan, D. Sek, *Prog. Polym. Sci.* **2011**, *36*, 1277; b) H. J. Yen, G. S. Liou, *Polym. Chem.* **2012**, *3*, 255; c) H. J. Yen, C. J. Chen, G. S. Liou, *Adv. Funct. Mater.* **2013**, *23*, 5307; d) Z. Ning, H. Tian, *Chem. Commun.* **2009**, 5483.

[19] C. W. Hu, K. M. Lee, K. C. Chen, L. C. Chang, K. Y. Shen, S. C. Lai, T. H. Kuo, C. Y. Hsu, L. M. Huang, R. Vittal, K. C. Ho, *Sol. Energy Mater. Sol. Cells* **2012**, *99*, 135.

[20] H. J. Yen, S. M. Gu, G. S. Liou, J. C. Chung, Y. C. Liu, Y. F. Lu, Y. Z. Zeng, *J. Polym. Sci., Part A: Polym. Chem.* **2011**, *49*, 3805.

[21] H. Y. Lin, G. S. Liou, *J. Polym. Sci., Part A: Polym. Chem.* **2009**, *47*, 285.